Article summary line: Evidence of SARS-CoV-2 exposure and infection detected in free-ranging white-tailed in southern Québec, Canada

Running title: SARS-CoV-2, White-tailed deer, Québec

Key words: SARS-CoV-2, COVID-19, White-Tailed Deer, Québec, Canada, Infection, Serology, Wildlife, Genomics

Title: First detection of SARS-CoV-2 infection in Canadian wildlife identified in free-ranging white-tailed deer (*Odocoileus virginianus*) from southern Québec, Canada

Authors: Jonathon D. Kotwa, Ariane Massé*, Marianne Gagnier, Patryk Aftanas, Juliette Blais-Savoie, Jeff Bowman, Tore Buchanan, Hsien-Yao Chee, Antonia Dibernardo, Peter Kruczkiewicz, Kuganya Nirmalarajah, Catherine Soos, Lily Yip, L. Robbin Lindsay, Oliver Lung, Bradley Pickering*, Samira Mubareka*

Affiliations: Sunnybrook Research Institute, Toronto, Ontario, Canada (J.D. Kotwa, P Aftanas, J. Blais-Savoie, H.Y. Chee, K. Nirmalarajah, L. Yip, S. Mubareka); Ministère des Forêts, de la Faune et des Parcs, Québec City, Québec, Canada (A. Massé, M. Gagnier); Wildlife Research and Monitoring Section, Ontario Ministry of Northern Development, Mines, Natural Resources and Forestry, Peterborough, Ontario, Canada (J. Bowman, T. Buchanan); Global Health Research Center and Division of Natural and Applied Sciences, Duke Kunshan University, Kunshan, Jiangsu, China (H.Y. Chee); National Microbiology Laboratory, Public Health Agency of Canada, Winnipeg (A. Dibernardo, L.R. Lindsay); National Centre for Foreign Animal Disease, Canadian Food Inspection Agency, Winnipeg, Manitoba, Canada (P. Kruczkiewicz, O.

Lung, B. Pickering); Ecotoxicology and Wildlife Health Division, Environment and Climate Change Canada, Saskatoon, Saskatchewan (C. Soos); Department of Veterinary Pathology, Western College of Veterinary Medicine, University of Saskatchewan, Saskatoon (C. Soos); Department of Biological Sciences, University of Manitoba, Winnipeg (O. Lung); Department of Veterinary Microbiology and Preventative Medicine, College of Veterinary Medicine, Iowa State University, Ames, Iowa, USA (B. Pickering); Department of Medical Microbiology and Infectious Diseases, University of Manitoba, Winnipeg (B. Pickering); Department of Laboratory Medicine and Pathobiology, University of Toronto, Toronto (S. Mubareka)

* Co-corresponding authors: Email: samira.mubareka@sunnybrook.ca (S. Mubareka); bradley.pickering@canada.ca (B. Pickering); ariane.masse@mffp.gouv.qc.ca (A. Massé)

Abstract

White-tailed deer are susceptible to SARS-CoV-2 and represent a relevant species for surveillance. We investigated SARS-CoV-2 infection in white-tailed deer in Québec, Canada. In November 2021, 251 nasal swabs and 104 retropharyngeal lymph nodes from 258 deer were analyzed for SARS-CoV-2 RNA, whole genome sequencing and virus isolation and 251 thoracic cavity fluid samples were tested for neutralizing antibodies. We detected SARS-CoV-2 RNA in three nasal swabs from the Estrie region and virus was isolated from two samples; evidence of past exposure was detected among deer from the same region. Viral sequences were assigned to lineage AY.44, a sublineage of B.1.617.2. All deer sequences clustered with human GISAID sequences collected in October 2021 from Vermont USA, which borders the Estrie region. Mutations in the S-gene and a deletion in ORF8 encoding a truncated protein were detected. These findings underscore the importance of ongoing surveillance of key wildlife species for SARS-CoV-2.

Main text

The emergence and rapid spread of coronavirus disease 2019 (COVID-19) caused by Severe Acute Respiratory Coronavirus 2 (SARS-CoV-2) has sparked concerns of spillover to susceptible wildlife populations, raising the possibility that new wildlife species could ultimately serve as virus reservoirs. In silico modelling of angiotensin-converting enzyme 2 (ACE2) receptor binding domain across possible host species suggests that cervids, cetaceans, primates, and some rodents are at highest risk for infection due to predicted binding with the SARS-CoV-2 spike protein [1]. Experimental studies have also revealed that wildlife species are susceptible to SARS-CoV-2 infection, including raccoons (*Procyon lotor*), striped skunks (*Mephitis mephitis*), North American deer mice (*Peromyscus maniculatus*), and white-tailed deer (*Odocoileus virginianus*) [2–5].

Evidence of natural infections of SARS-CoV-2 have been reported in captive and wild animals, including farmed and free-living American mink *(Neogale vison)* [6–8]. Evidence of mink-to-human transmission has also been described from captive mink in Denmark [9]. This raises concerns about the establishment of an animal reservoir for the virus.

Surveillance of SARS-CoV-2 in wildlife is ongoing in Canada and is conducted using a One Health approach; One Health recognizes that human and animal health are interconnected and balances concerns for both human and animal health [10]. Through collaborative efforts between governmental and academic research groups and with a focus on peri-domestic species, 776 animals from 17 different wildlife species (e.g., raccoon, skunk, mink), have been tested to date in the provinces of Ontario and Québec [11]**.** Although no evidence of SARS-CoV-2 RNA was found in these animals, continued surveillance of wildlife species is important as variants of concern (VOCs) emerge and host ranges potentially broaden or shift.

As the pandemic progresses, new evidence is emerging regarding susceptible wildlife that may act as competent reservoirs for SARS-CoV-2. White-tailed deer (WTD) are now considered a highly relevant species as a result of experimental evidence of susceptibility in addition to recent evidence of SARS-CoV-2 exposure and infection, across the northeastern USA [5,12–16]. In light of this emerging evidence and concerns for the establishment of a wildlife reservoir for SARS-CoV-2, we investigated SARS-CoV-2 in WTD in southern Québec, Canada as part of a broader pan-Canadian approach to investigate SARS-CoV-2 spillover into wildlife. We also employ viral genomics and isolation to further characterize SARS-CoV-2 infection in this species.

Materials and Methods

Sample Collection and Study Region

White-tailed deer were sampled during the scheduled hunting season after harvesting by licensed hunters. Samples were collected at two big game registration stations in Dunham and Brownsburg (Figure 1); the Brownsburg station included collection of retropharyngeal lymph node (RPLN) tissues for Chronic Wasting Disease surveillance conducted by the Ministère des Forêts, de la Faune et des Parcs (MFFP) in free-ranging WTD Québec in early November 2021 [17]. Notably, these two areas of southern Québec have contrasting deer density: 1) the Laurentides region is characterized by low deer density (~1 deer/km^2), and 2) the Estrie region is characterized high deer density (13–15 deer/km^2) (MFFP, unpublished data). We collected nasal swabs in 1 mL universal transport media and retropharyngeal lymph node (RPLN) tissues were collected in dry 2 mL tubes; both sample types were stored at -80°C prior to analysis. Additionally, thoracic cavity fluid was collected; filter paper strips designed to absorb 100 µl of liquid, or the equivalent of 40 µL of serum (Nobuto filter paper strips, Advantec, MFS,

Pleasanton, CA, USA) were submerged in thoracic cavity fluid (i.e., a mixture of fluid exudate and blood), allowed to dry at room temperature, placed in individual manila envelopes, and stored at -20°C prior to testing. Geographic location of origin and demographic data for each animal were also recorded when available.

RNA Extraction and PCR

RNA extraction and PCR testing were performed at the Sunnybrook Research Institute (SRI) in Toronto, Ontario. RNA extractions were performed using 140 µL of nasal swab sample spiked with Armored RNA enterovirus (Asuragen; https://www.asuragen.com) via the Nuclisens EasyMag using Generic Protocol 2.0.1 (bioMérieux Canada Inc., St-Laurent, QC, Canada) according to manufacturer's instructions. Tissue samples were thawed, weighed, minced with a scalpel, and homogenized in 600 µL of lysis buffer using the Next Advance Bullet Blender (Next Advance, Troy, NY, USA) and a 5 mm stainless steel bead at 5 m/s for 3 minutes. RNA from 30 mg tissue samples was extracted via the Nuclisens EasyMag using Specific Protocol B 2.0.1; RNA was eluted in 50 µL. Reverse-transcription polymerase chain reaction (RT-PCR) was performed using the Luna Universal Probe One-Step RT-qPCR kit (New England BioLabs; https://www.neb.ca). Two gene targets were used for SARS-CoV-2 RNA detection: the 5' untranslated region (UTR) and the envelope (E) gene [18]. The cycling conditions were: 1 cycle of denaturation at 60°C for 10 minutes then 95°C for 2 minutes followed by 44 amplification cycles of 95°C for 10 seconds and 60°C for 15 seconds. Quantstudio 3 software (Thermo Fisher Scientific; https://www.thermofisher.com) was used to determine cycle threshold (Ct). All samples were run in duplicate and samples with Ct <40 for both gene targets in at least one replicate were considered presumed positive.

Original material from presumed positive samples detected at SRI were sent to the Canadian Food Inspection Agency (CFIA) for confirmatory PCR testing. Total RNA spiked with Armored RNA enterovirus was extracted using the MagMax CORE Nucleic Acid Purification Kit (ThermoFisher Scientific) and the automated KingFisher Duo Prime magnetic extraction system. The enteroviral armored RNA was used as an exogenous extraction control. Confirmatory RT-qPCR was performed using primers and probe specific for both SARS-CoV-2 E and nucleocapsid (N) genes [19]. Master mix for qRT-PCR was prepared using TaqMan Fast Virus 1-step Master Mix (ThermoFisher Scientific) according to manufacturer's instructions. Reaction conditions were 50°C for 5 minutes, 95°C for 20 seconds, and 40 cycles of 95°C for 3 seconds then 60°C for 30 seconds. Runs were performed by using a 7500 Fast Real-Time PCR System (Thermofisher, ABI). Samples with Ct <36 for both gene targets were considered positive.

SARS-CoV-2 amplification and sequencing

SARS-CoV-2 whole genome sequencing was performed at SRI and analyzed at CFIA. All presumed PCR positive samples were analyzed. Extracted RNA was reverse transcribed into cDNA; 8 µL RNA was mixed with 8 µL nuclease-free water and 4 µL LunaScript RT SuperMix (New England BioLabs) then incubated at 25°C for 2 minutes followed by an incubation at 55°C for 20 minutes and 95°C for 1 minute before holding at 4°C.

cDNA was amplified using ARTIC v3 primer pools (https://github.com/artic-network/artic-ncov2019). Two separate reactions were prepared by combining 2.5 µL cDNA with 6 µL nuclease-free water, 12.5 µL Q5 Hot Start High-Fidelity 2X Master Mix (New England BioLabs) and 4 µL of 10 µM primer pool 1 or primer pool 2 (Integrated DNA Technologies; https://www.idtdna.com). The PCR cycling conditions included an initial

denaturation at 98°C for 30 seconds followed by 35 cycles of 98°C for 15 seconds and 63°C for 5 minutes before holding at 4°C. Both reactions were combined and purified with 1X ratio Sample Purification Beads (Illumina; https://www.illumina.com). The resulting amplicons were quantified using Qubit 1X dsDNA HS Assay Kit (Thermo Fisher Scientific).

Libraries were constructed using Illumina DNA Prep (Illumina) and IDT for Illumina DNA/RNA UD Indexes (Illumina) and sequenced on Illumina MiniSeq using 2x149 paired-end reads.

Paired-end Illumina reads for samples 4055, 4204, 4205 and 4249 were analyzed using the nf-core/viralrecon Nextflow workflow (v2.2) [20–22], which performed the following analysis steps: FastQC (v0.11.9) read quality assessment (https://www.bioinformatics.babraham.ac.uk/projects/fastqc/); fastp (v0.20.1) read quality filtering and trimming [23]; read mapping to Wuhan-Hu-1 (MN908947.3) SARS-CoV-2 reference sequence with Bowtie2 (v2.4.2) [24]; read mapping statistics calculation with Mosdepth (v0.3.1) [25] and Samtools (v1.12) [26,27]; ARTIC V3 primer trimming, variant calling and consensus sequence generation with iVar (v1.3.1) [28]; variant effect analysis and summarization with SnpEff (v5.0) [29] and SnpSift (v4.3t) [30], respectively; SARS-CoV-2 lineage assignment with Pangolin (v3.1.17).

Phylogenetic analysis was performed with the WTD consensus sequences generated by nf-core/viralrecon and GISAID [31–33] sequences (downloaded 2021-12-14 from https://www.gisaid.org/) belonging to the same AY.44 Pangolin lineage as the WTD sequences using the CFIA-NCFAD/scovtree Nextflow workflow (v1.6.0) (https://github.com/CFIA-NCFAD/scovtree/). The following analysis steps were performing as part of the CFIA-NCFAD/scovtree workflow: WTD consensus sequences from nf-core/viralrecon (v2.2) analysis were assigned to a Pangolin lineage using Pangolin (v3.1.17); GISAID sequences were filtered

for up to 100,000 total sequences from Canada and the USA and belonging to the same Pangolin lineages as the WTD sequences; Nextalign CLI (v0.2.0) [34] multiple sequence alignment (MSA) of WTD and filtered GISAID sequences; down-sampling of Nextalign MSA to 20,000 sequences for phylogenetic tree inference preferentially filtering for MSA sequences with the least gaps and Ns and from Canada (due to the WTD samples being collected in Canada and to reduce the bias from a large proportion of GISAID sequences being from the USA); IQ-TREE (v2.1.4-beta) [35,36] phylogenetic analysis with the GTR model [37]; pruning of the 20,000 taxa IQ-TREE phylogenetic tree with BioPython [38] down to 50 taxa (outgroup Wuhan-Hu-1 reference strain (MN908947.3), 4 WTD taxa and 45 GISAID taxa most closely related to WTD sequences) for visualization; Nextclade CLI (v0.14.4) [34] analysis to identify amino acid substitutions and deletions in WTD and GISAID sequences.

Virus Isolation

Virus isolation was performed on PCR-positive nasal swabs in containment level 3 at the University of Toronto. Vero E6 cells were seeded at a concentration of $3x10^5$ cells/well in a six well-plate. The next day, 250 µL of sample with 16 µg/mL TPCK-treated trypsin (New England BioLabs), 2X penicillin and streptomycin and 2X antibiotic-antimycotic (Wisent; https://www.wisentbioproducts.com/en/) was inoculated onto cells. Plates were returned to a 37°C, 5% CO_2 incubator for 1 hour and rocked every 15 minutes. After 1 hour, the inoculum was removed and replaced with DMEM containing 2% FBS, 6 µg/mL TPCK-treated trypsin, 2X Pen/Strep, and 2X antibiotic-antimycotic. Cells were observed daily under a light microscope for cytopathic effect for 5 days post infection. The RT-PCR assay and sequencing method described above were used to confirm SARS-CoV-2 isolation from supernatant.

Serology

Antibody testing on thoracic cavity fluid samples was performed at the National Microbiology Laboratory, Public Health Agency of Canada in Winnipeg, Manitoba. To obtain the 1:9 dilution required for testing, saturated Nobuto strips were cut into 4–5 pieces and placed into a 2 mL tube containing 360 µL phosphate buffered saline (PBS) pH 7.4 and eluted overnight at 4°C. For strips that were not fully saturated, the volume of PBS was adjusted proportionately. Eluted samples were mixed by vortexing and tested using the GenScript cPass™ SARS-CoV-2 Neutralization Antibody Detection Kit (GenScript USA, Inc. Piscataway, NJ, USA) according to the manufacturer's protocol.

Briefly, 60 µL of a sample was added to 60 µL HRP-conjugated RBD solution and incubated at 37°C for 30 minutes. A 100 µL aliquot of the mixture was transferred to the ELISA microwell test plate and incubated at 37°C for 15 minutes. Microwells were washed 4 times with 260 µL wash buffer then 100 µL TMB substrate was added to each well. Following a 20-minute incubation in the dark at room temperature, 50 µL of Stop Solution was added to each well. Absorbance was read immediately at 450 nm. Each assay plate included positive and negative controls that met required quality control parameters. Percentage inhibition was calculated for each sample using the following equation:

Percent Inhibition = (1- Optical Density Sample/Optical Density Negative Control) x100%

Samples with greater than or equal to 30% inhibition were considered positive for SARS-CoV-2 neutralizing antibodies.

Statistical analyses

Confidence intervals (CI) for SARS-CoV-2 prevalence of infection and exposure were estimated using the Agresti-Coull CI method [39]. Diagnostic data were plotted on a map of southern Québec according to the latitude and longitude of each WTD with human population density [40] and deer harvesting density data [41]. Graphic displays were produced via QGIS 2.18.23 (Quantum GIS Development Team; http://www.qgis.org). All statistical analyses were conducted using Stata/SE 15.1 (StataCorp, College Station, Texas, USA; http://www.stata.com).

Results

From November 6–8 2021, 258 WTD were sampled in two areas from southern Québec, Canada. The majority of the sampled WTD were adults (92%) and males (79%). We collected 251 nasal swabs and 104 RPLNs and tested for the presence of SARS-CoV-2 RNA via RT-PCR. Precise location data were obtained for 257 WTD.

Four nasal swabs were considered presumed PCR-positive by SRI, three of which were confirmed via the CFIA (Table 1). Of all nasal swabs, 1.2% (3/251; 95% CI 0.3–3.5%) were confirmed positive for SARS-CoV-2 RNA (Table 2); no RPLNs were positive. All positive deer were adults, and two of the three positives were male. The three confirmed SARS-CoV-2-positive deer were harvested through regulated hunting activity in the higher deer density region (Estrie) (Figure 2b). Two of the three confirmed SARS-CoV-2-positive nasal swabs yielded viable virus (Figure 3). Notably, no RPLNs were collected from deer with SARS-CoV-2 positive nasal swabs.

High-throughput sequencing conducted on swab 4055, 4205, and 4249 obtained genome coverage of over 95% with equal to or greater than 10X coverage and 69.1% genome coverage and at least 10X coverage (mean depth of 116.5) was obtained for the higher Ct swab 4204 (Table 3). Sequences from all three CFIA-confirmed positive WTD were classified as belonging

to the 21A Delta clade with Nextclade. Sequences from 4055, 4205, and 4249 were assigned to lineage AY.44, a sublineage of B.1.1.617.2, with Pangolin (0.96-0.99 ambiguity score), while 4204 could not be confidently assigned to a Pangolin lineage due to the large number of N bases (31%) in the consensus sequence. Phylogenetic analysis reveals that all sequenced samples cluster together and shared a most recent common ancestor with GISAID sequences from Vermont, USA collected between 2021-10-14 and 2021-10-27 (Figure 4).

Mutations were observed in the four presumed positive WTD samples (Table 4). Notably, two S gene mutations were observed in the WTD sequences that were not observed in closely related AY.44 sequences from GISAID: S:T22I in samples 4055, 4205 and the partial genome of 4204; S:A27V in sample 4055 only. The S:T22I mutation has been observed in 10,395 GISAID sequences as of 2021-12-13 from a multitude of lineages with the B.1.1.487 lineage having the highest prevalence of the mutation (153/174 sequences (88%)). The S:A27V mutation has been observed in 4,009 GISAID sequences as of 2021-12-13 with the highest prevalence in the B.1.1.618 lineage (10/40 sequences (25%)). The S:G142D mutation, which is present in 61% of AY.44 sequences in GISAID (122,028/200,599 sequences as of 2021-12-13), is present in samples 4055 and 4249 as a minor variant (57% and 53% allele fraction, respectively). The S:G142D mutation is prevalent in many Delta sublineage sequences and present in 2,132,548 GISAID sequences as of 2021-12-13. Interestingly, the S:G1085R mutation, which is present in all four sequenced samples and related AY.44 sequences, is only present in 0.12% (246/200,599) in lineage AY.44 and has been identified in 706 GISAID sequences as of 2021-12-13.

An inframe deletion leading to a stop codon in the ORF8 was observed at S67/K68 (TCTA to T deletion at nucleotide position 28,092) in sample 4205. Additionally, an ORF8 inframe deletion of 6 amino acids at positions 61–66 and L60F mutation were observed in

sample 4205 although with an allele fraction of 59% (262/442 observations of TGTGCGTGGATGAGGCTGG to T at nucleotide position 28,072). High variability and truncation of ORF8 arising from nonsense mutations and deletions has been observed previously, underscoring the potential role of ORF8 in SARS-CoV-2 adaptation [42,43].

A total of 251 thoracic cavity fluid samples were tested for SARS-CoV-2 neutralizing antibodies. Overall, we found evidence of neutralizing antibodies to SARS-CoV-2 in 5.6% (14/251; 95% CI 3.3–9.2%) thoracic cavity fluid samples; all but one (93%) were adults and nine (64%) were males. All seropositive WTD were identified in the Estrie region (Table 1; Figure 2). No WTD were both PCR and antibody positive.

Discussion

The first evidence of SARS-CoV-2 infection in WTD came on the tails of widespread evidence of exposure in this species across the northeastern USA [12]. First reported in Iowa [15], followed by evidence from Ohio [14], SARS-CoV-2 infection in WTD appeared to be widespread and has been speculated to have resulted from multiple spillover events from humans. Most recently, evidence of exposure in both captive and free-ranging deer has now been reported in Texas, extending the known geographic range in North America [16,44]. In this report, we describe the first detection of SARS-CoV-2 exposure and infection in WTD in Canada. Overall, SARS-CoV-2 was detected in 1.2% (95% CI 0.2–3.6%) of the nasal swabs from sampled deer and neutralizing antibodies against SARS-CoV-2 were detected in 5.6% (95% CI 3.3–9.2%). Notably, the prevalence of infection of SARS-CoV-2 in WTD described in the present study is much lower than what was reported in Iowa (33.2%) and Ohio (35.8%) [14,15]. Similarly, our described seroprevalence is substantially lower than the 40% reported for the northeastern USA,

or the 37% reported from Texas [12,44]. This observation may suggest that spillover of SARS-CoV-2 to WTD in this region of Québec is a recent occurrence.

Based on the currently available data of SARS-CoV-2 in WTD, exposure and infection appear to be temporally and geographically clustered. Chandler and colleagues found that seroprevalence was highly clustered by individual counties, with nearly half of sampled counties showing no evidence of exposure [12]. Kuchipudi and colleagues found a temporal increase in prevalence of infection beginning in November 2020 and continuing to January 2021 [15]. It is possible that these observed temporal and spatial patterns are interconnected and, in part, a result of WTD ecology. It is unclear how this temporal pattern relates to human cases. Notably, both aforementioned studies conducted sample collection over periods of time that corresponded to or followed major pandemic peaks in humans in their respective regions [12,15]. Therefore, more longitudinal surveillance of SARS-CoV-2 in WTD is needed to understand the epidemiology of the virus in this species.

All PCR- and seropositive WTD were identified in the Estrie region (Table 1; Figure 2). While unsurprising given the apparent spatial clustering of SARS-CoV-2 in WTD, this may also be due to several factors: 1) WTD population density and hunter harvest are greater in Estrie (13-15 deer/km^2) compared to the Laurentides (~1 deer/km^2) (MFFP, unpublished data), 2) the sampled regions in Estrie have higher human population density compared to sampled regions in the Laurentides (Figure 2a), and 3) COVID-19 positivity in humans was greater in Estrie (4.2%) during the study period compared to the Laurentides (2.3%)[45]. Although we included SARS-CoV-2 sequences from humans from Québec, no sequences were available from the Estrie region and may represent regional under sampling of SARS-CoV-2 sequences from humans. It is

interesting to note that the Estrie region borders Vermont, USA but, to the authors' knowledge, no evidence of SARS-CoV-2 in WTD has been reported in Vermont to date.

Susceptibility of WTD to SARS-CoV-2 and evidence of deer-to-deer transmission raise concerns about the development of a reservoir for the virus in this species [5,46]. From a public health perspective, a wildlife reservoir for SARS-CoV-2 is troubling as it would be inherently much more difficult to control outbreaks in the human population. Additionally, the spread of SARS-CoV-2 through animal populations could further contribute to the development of VOCs, potentially undermining the efficacy of medical countermeasures such as antivirals and vaccines [47–49]. In the present work, whole SARS-CoV-2 genome sequences were found to contain two S gene mutations (S:T22I and S:A27V) that were different between the deer and from the most closely related AY.44 sequences from GISAID. This observation raises the possibility of transboundary transmission and that SARS-CoV-2 has been circulating in WTD for some time and may be useful genetic markers for tracking the transmission and evolution of SARS-CoV-2 in future study of WTD and human sequences. However, it is not clear if these changes have broader public health implications. Further work is needed to determine if WTD could become a reservoir for SARS-CoV-2. Specifically, more longitudinal studies are needed to support persistence and maintenance of SARS-CoV-2 in WTD populations [50].

It is presently unclear how the deer acquired SARS-CoV-2 infection. Anthropogenic settings are suggested to provide opportunities for direct and indirect contact with humans and human contaminated sources [2,14,51]. Perhaps captive deer may play a role as SARS-CoV-2 exposure in captive deer has been documented and contacts between free-ranging and captive deer have been observed [16,17]. Wastewater has also been postulated as a potential route of transmission to susceptible wildlife; SARS-CoV-2 is shed in human feces and has been detected

in wastewater and urban run-off [52,53]. However, this route of transmission has yet to be conclusively demonstrated in the absence of evidence of infectious virus in water [54].

Viral isolation is used to demonstrate presence of viable virus in the sample. Notably, we successfully isolated viable SARS-CoV-2 from two of the three CFIA-confirmed PCR-positive nasal swabs. Based on previous experimental work, productive viral replication is limited to the upper respiratory tract with shedding of infectious virus in nasal secretions of infected WTD [5,13]. While no current evidence of SARS-CoV-2 spillback from deer to humans exists, these findings warrant increased awareness of the risks associated with human contact with free-living and captive WTD. While detecting SARS-CoV-2 in secretions or tissues, and evidence of viral isolation provides support that transmission to humans could occur, observational evidence of deer-to-human transmission is absent. In addition, although there are no clear signs of disease among infected deer, the implications for wildlife health remain unknown. Further viral adaptations have led to enhanced disease in humans; close follow-up is required to ensure deer health is not impacted.

There are several limitations for this study that should be considered. First, while leveraging the regular WTD hunting season resulted in a large number of samples, the present work was conducted over a short time period and a relatively small geographic region. Therefore, our study represents a snapshot in time and space. Future work should aim to obtain longitudinal data to investigate maintenance of SARS-CoV-2 in Québec WTD populations and assess for spatiotemporal patterns in pathogen ecology. Second, samples analyzed in this study were derived from harvested deer and were therefore collected post-mortem. Although 98% of samples were collected within 48 hours of harvest, it is possible that inhibitors or sample degradation occurred between harvest and sample collection. Lastly, our study only focuses on

free-ranging WTD populations and we therefore cannot make inferences about SARS-CoV-2 in captive conspecifics.

At the time of writing, surveillance is currently ongoing across Canada. Our findings underscore that further surveillance efforts in WTD in Québec and across Canada are warranted. Further work is needed to understand how the virus is transmitted from humans to deer, how efficiently and sustainably the virus is transmitted among deer in a natural setting, if WTD could ultimately serve as a reservoir for SARS-CoV-2 in Canada, how viral adaptations occur in WTD, and if and how frequently is deer-to-human transmission occurring. Ongoing coordinated and cross-disciplinary efforts are required to ensure a One Health approach is applied to this critical pandemic challenge by informing evidence-based decision-making for human and animal health.

Acknowledgements

Many thanks to the southern Québec hunters, the technicians and biologists who assisted with sample collection (Matthew Rokas-Bérubé, Yannicia Fréchette-Hudon, Catherine Greaves, Charles-Étienne Gagnon, Marylou Meyer, Camille Klein, Stéphane Lamoureux, Yannick Bilodeau, François Lebel, Sophie Plante, and Isabelle Laurion), and the technicians that assisted with sample analysis (Emily Chien, Mathieu Pinette, Winfield Yim, and Nikki Toledo). We are grateful for the work of D. Bulir in developing for the UTR gene target used in the Sunnybrook Research Institute PCR analysis. Ms Nikki Toledo from the National Microbiology Laboratory performed the serological testing on the thoracic cavity samples analyzed in this study.

References:

1. Damas, J. et al. Broad host range of SARS-CoV-2 predicted by comparative and structural analysis of ACE2 in vertebrates. *Proc. Natl. Acad. Sci*. **117**, 22311–22322 (2020).

2. Bosco-Lauth, A. M. et al. Peridomestic Mammal susceptibility to severe acute respiratory syndrome coronavirus 2 infection. *Emerg. Infect. Dis.* **27**, 2073–2080 (2021).

3. Francisco, R. et al. Experimental susceptibility of North American raccoons (*Procyon lotor*) and striped skunks (*Mephitis mephitis*) to SARS-CoV-2. Preprint at *bioRxiv*. https://www.biorxiv.org/content/10.1101/2021.03.06.434226v1 (2021).

4. Griffin, B. D. et al. SARS-CoV-2 infection and transmission in the North American deer mouse. *Nat. Commun*. **12**, 3612 (2021).

5. Palmer, M. V. et al. Susceptibility of White-Tailed Deer (*Odocoileus virginianus*) to SARS-CoV-2. *J. Virol.* **95**, e00083-21 (2021).

6. Aguiló-Gisbert, J. et al. First description of SARS-CoV-2 infection in two feral American Mink (*Neovison vison*) caught in the wild. *Animals* **11**, 1422 (2021).

7. Oreshkova, N. et al. SARS-CoV-2 infection in farmed Minks, the Netherlands, April and May 2020. *Eurosurveillance* **25**, 2001005 (2020).

8. Shriner, S. A. et al. SARS-CoV-2 Exposure in escaped mink, Utah, USA. *Emerg. Infect. Dis*. **27**, 988–990 (2021).

9. Hammer, A. S. et al. SARS-CoV-2 Transmission between Mink (*Neovison vison*) and Humans, Denmark. *Emerg. Infect. Dis.* **27**, 547–551 (2021).

10. Delahay, R. J. et al. Assessing the risks of SARS-CoV-2 in wildlife. *One Health Outlook* **3**, 7 (2021).

11. Greenhorn, J. E. et al. SARS-CoV-2 wildlife surveillance in Ontario and Québec, Canada. Preprint at *bioRvix*. https://www.biorxiv.org/content/10.1101/2021.12.02.470924v1 (2021).

12. Chandler, J. C. et al. SARS-CoV-2 exposure in wild White-Tailed Deer (*Odocoileus virginianus*). *Proc. Natl. Acad. Sci.* **118**, (2021).

13. Cool, K. et al. Infection and transmission of ancestral SARS-CoV-2 and its alpha variant in pregnant White-Tailed Deer. *Emerg. Microbes Infect.* **0**, 1–39 (2021).

14. Hale, V. L. et al. SARS-CoV-2 infection in free-ranging white-tailed deer. *Nature* 1–8 (2021).

15. Kuchipudi, S. V. et al. Multiple spillovers and onward transmission of SARS-Cov-2 in free-living and captive White-tailed deer (*Odocoileus virginianus*). Preprint at *bioRvix*. https://www.biorxiv.org/content/10.1101/2021.10.31.466677v1 (2021).

16. Roundy, C. M. et al. High seroprevalence of SARS-CoV-2 in white-tailed deer (*Odocoileus virginianus*) at one of three captive cervid facilities in Texas. Preprint at *bioRvix*. https://www.biorxiv.org/content/10.1101/2022.01.05.475172v1 (2022).

17. Gagnier, M., Laurion, I. & DeNicola, A. J. Control and surveillance operations to prevent chronic wasting disease establishment in free-ranging White-Tailed Deer in Québec, Canada. *Animals* **10**, 283 (2020).

18. LeBlanc, J. J. et al. Real-time PCR-based SARS-CoV-2 detection in Canadian laboratories. J. *Clin. Virol.* **128**, 104433 (2020).

19. Lu, X. et al. US CDC Real-time reverse transcription PCR panel for detection of severe acute respiratory syndrome coronavirus 2. *Emerg. Infect. Dis*. **26**, 1654–1665 (2020).

20. Ewels, P. A. et al. The nf-core framework for community-curated bioinformatics pipelines. *Nat. Biotechnol.* **38**, 276–278 (2020).

21. Patel, H. et al. nf-core/viralrecon: nf-core/viralrecon v2.2 - Tin Turtle(2.2). *Zenodo* (2021). doi:10.5281/zenodo.5146252.

22. Tommaso, P. D. et al. Nextflow enables reproducible computational workflows. *Nat. Biotechnol.* **35**, 316–319 (2017).

23. Chen, S., Zhou, Y., Chen, Y. & Gu, J. fastp: an ultra-fast all-in-one FASTQ preprocessor. *Bioinformatics* **34**, i884–i890 (2018).

24. Langmead, B. & Salzberg, S. L. Fast gapped-read alignment with Bowtie 2. *Nat. Methods* **9**, 357–359 (2012).

25. Pedersen, B. S. & Quinlan, A. R. Mosdepth: quick coverage calculation for genomes and exomes. *Bioinformatics* **34**, 867–868 (2017).

26. Danecek, P. et al. Twelve years of SAMtools and BCFtools. *GigaScience* **10**, giab008 (2021).

27. Li, H. et al. The Sequence Alignment/Map format and SAMtools. *Bioinformatics* **25**, 2078–2079 (2009).

28. Grubaugh, N. D. et al. An amplicon-based sequencing framework for accurately measuring intrahost virus diversity using PrimalSeq and iVar. *Genome Biol.* **20**, 8 (2019).

29. Cingolani, P. et al. A program for annotating and predicting the effects of single nucleotide polymorphisms, SnpEff: SNPs in the genome of Drosophila melanogaster strain w1118; iso-2; iso-3. *Fly (Austin)* **6**, 80–92 (2012).

30. Cingolani, P. et al. Using Drosophila melanogaster as a model for genotoxic chemical mutational studies with a new program, SnpSift. *Front. Genet.* **3**, 35 (2012).

31. Elbe, S. & Buckland□Merrett, G. Data, disease and diplomacy: GISAID's innovative contribution to global health. *Glob. Chall.* **1**, 33–46 (2017).

32. Khare, S. et al. GISAID's role in pandemic response. *China CDC Wkly*. **3**, 1049–1051 (2021).

33. Shu, Y. & McCauley, J. GISAID: Global initiative on sharing all influenza data – from vision to reality. *Eurosurveillance* **22**, 30494 (2017).

34. Aksamentov, I., Roemer, C., Hodcroft, E. B. & Neher, R. A. Nextclade: clade assignment, mutation calling and quality control for viral genomes. *J. Open Source Softw*. **6**, 3773 (2021).

35. Minh, B. Q. et al. IQ-TREE 2: New models and efficient methods for phylogenetic inference in the genomic era. *Mol. Biol. Evol.* **37**, 1530-34 (2020).

36. Nguyen, L.-T., Schmidt, H. A., von Haeseler, A. & Minh, B. Q. IQ-TREE: A fast and effective stochastic algorithm for estimating maximum-likelihood phylogenies. *Mol. Biol. Evol*. **32**, 268–274 (2014).

37. Tavaré, S. Some probabilistic and statistical problems in the analysis of DNA sequences. *Lect. Math. Life Sci.* **17**, 57–86 (1986).

38. Cock, P. J. A. et al. Biopython: freely available Python tools for computational molecular biology and bioinformatics. *Bioinformatics* **25**, 1422–1423 (2009).

39. Agresti, A. & Coull, B. A. Approximate is better than "exact" for interval estimation of binomial proportions. *Am. Stat.* **52**, 119–126 (1998).

40. Statistics Canada. Population and dwelling count highlight tables, 2016 Census [cited 2021 Dec 07]. https://www12.statcan.gc.ca/census-recensement/2016/dp-pd/hlt-fst/pd-pl/Table.cfm?Lang=Eng&T=101&S=50&O=A#2016A000224

41. Ministère des Forêts, de la Faune et des Parcs (MFFP). Season 2020 - White-tailed deer harvest per hunting zone. (2020).

42. Fahmi, M., Kitagawa, H., Yasui, G., Kubota, Y. & Ito, M. The functional classification of ORF8 in SARS-CoV-2 replication, immune evasion, and viral pathogenesis inferred through phylogenetic profiling. *Evol. Bioinforma. Online* **17**, 11769343211003080 (2021).

43. Pereira, F. Evolutionary dynamics of the SARS-CoV-2 ORF8 accessory gene. *Infect. Genet. Evol.* **85**, 104525 (2020).

44. Palermo, P. M., Orbegozo, J., Watts, D. M. & Morrill, J. C. SARS-CoV-2 neutralizing antibodies in White-Tailed Deer from Texas. *Vector-Borne Zoonotic Dis.* **22**, 62-64 (2021).

45. Institut national de & santé publique du Québec (INSPQ). Données COVID-19 par région sociosanitaire [cited 2021 Dec 07]. https://www.inspq.qc.ca/covid-19/donnees/par-region

46. Martins, M. et al. From Deer-to-Deer: SARS-CoV-2 is efficiently transmitted and presents broad tissue tropism and replication sites in White-Tailed Deer. Preprint at *bioRvix*. https://www.biorxiv.org/content/10.1101/2021.12.14.472547v1 (2021).

47. Bashor, L. et al. SARS-CoV-2 evolution in animals suggests mechanisms for rapid variant selection. Preprint at bioRvix. https://www.biorxiv.org/content/10.1101/2021.03.05.434135v2 (2021).

48. Larsen, H. D. et al. Preliminary report of an outbreak of SARS-CoV-2 in mink and mink farmers associated with community spread, Denmark, June to November 2020. *Eurosurveillance* **26**, 2100009 (2021).

49. Wei, C. et al. Evidence for a mouse origin of the SARS-CoV-2 Omicron variant. *J. Genet. Genomics* (2021).

50. Haydon, D., Cleveland, S., Taylor, L. & Laurenson, M. Identifying Reservoirs of Infection: A Conceptual and Practical Challenge. *Emerg. Infect. Dis.* **8**, 1468–1473 (2002).

51. Franklin, A. B. & Bevins, S. N. Spillover of SARS-CoV-2 into novel wild hosts in North America: A conceptual model for perpetuation of the pathogen. *Sci. Total Environ.* **733**, 139358 (2020).

52. Bivins, A. et al. Persistence of SARS-CoV-2 in water and wastewater. *Environ. Sci. Technol. Lett.* **7**, 937–942 (2020).

53. Manuel, D. G. et al. The role of wastewater testing for SARS-CoV-2 surveillance. *Science Briefs of Ontario COVID-19 Science Advisory Table* **2** (2021).

54. Giacobbo, A., Rodrigues, M. A. S., Zoppas Ferreira, J., Bernardes, A. M. & de Pinho, M. N. A critical review on SARS-CoV-2 infectivity in water and wastewater. What do we know? *Sci. Total Environ.* **774**, 145721 (2021).

Table 1. The cycle threshold (Ct) value results for the presumptive positive deer nasal swab samples from southern Québec, Canada, November 6-8 2021

	Sunnybrook Research Institute*			Canadian Food Inspection Agency†		
Nasal Swab ID	UTR Ct	E Ct	Result	N2 Ct	E Ct	Result
4055	21.42	20.30	Positive	15.75	16.03	Positive
4204	33.92	35.879	Positive	36.95	35.96	Negative
4205	28.61	29.03	Positive	33.08	32.36	Positive
4249	17.57	19.90	Positive	12.47	14.07	Positive

* Two gene targets were used for SARS-CoV-2 RNA detection at the Sunnybrook Research Institute: the 5' untranslated region (UTR) and the envelope (E) gene [18].

† Confirmatory RT-qPCR was performed at the Canadian Food Inspection Agency using primers and probes specific for both SARS-CoV-2 envelope (E) and nucleocapsid (N) genes [19].

Table 2. Results from SARS-CoV-2 PCR testing of nasal swabs and retropharyngeal lymph node tissue, and antibody testing of thoracic cavity fluid from white-tailed deer, in two sampling regions, southern Québec, Canada, November 6-8 2021*

	Nasal Swabs		Retropharyngeal Lymph Nodes		Thoracic Cavity Fluid	
Sampling area	No. Tested	No. SARS-CoV-2 RNA Positive (%; 95% CI)	No. Tested	No. SARS-CoV-2 RNA Positive (%; 95% CI)	No. Tested	No. SARS-CoV-2 Antibody Positive (%; 95% CI)
Dunham station, Estrie region, High deer density	150	3 (2.0; 0.4–6.0)	NA	NA	150	14 (9.3; 5.5–15.2)
Browsburg station, Laurentides region, Low deer density	101	0 (0; 0–4.4)	104	0 (0; 0–4.3)	101	0 (0; 0–4.4)
Total	251	3 (1.2; 0.2–3.6)	104	0 (0; 0–4.3)	251	14 (5.6; 3.3–9.2)

*NA, not applicable.

Table 3. Read mapping statistics from nf-core/viralrecon analysis for four presumptive SARS-CoV-2 positive white-tailed deer nasal swab samples from southern Québec, Canada, November 6-8 2021

Nasal Swab ID*	Genome Coverage (%)†	Mean Coverage Depth	Total Reads	Mapped Reads	0X positions	<10X positions
4055	99.6	1227.1	375796	293802	121	121
4204	69.1	116.5	503532	29803	3219	9245
4205	95.8	1096.8	370802	252101	674	1255
4249	98.9	1894.8	583638	460000	69	314

* 4055, 4205, and 4249 were confirmed positive via the Canadian Food Inspection Agency SARS-CoV-2 PCR.

† Genome coverage was calculated as the proportion of Wuhan-Hu-1 (MN908947.3) reference positions with at least 10X read mapping depth.

Table 4. Summary of mutations leading to amino acid changes found in sequences from four presumptive SARS-CoV-2 positive white-tailed deer nasal swab samples from southern Québec, Canada, November 6-8 2021

Gene	Amino Acid Mutation	Nucleotide Mutation	Nasal Swab ID(s) [*]	Max Allele Fraction (%)[†]	Major Variant?[‡]
orf1ab	ΔM85	TATG517T	4204	88.9	Yes
orf1ab	V1143F	G3692T	4055; 4205; 4249	100	Yes
orf1ab	A1306S	G4181T	4055; 4204; 4205; 4249	100	Yes
orf1ab	Q1784H	G5617T	4055; 4204; 4205; 4249	100	Yes
orf1ab	L1853F	C5822T	4205	91.4	Yes
orf1ab	P2046L	C6402T	4055; 4205; 4249	100	Yes
orf1ab	H2125Y	C6638T	4055; 4204; 4205; 4249	100	Yes
orf1ab	S2224F	C6936T	4249	26.1	No
orf1ab	S2242F	C6990T	4204; 4205	100	Yes
orf1ab	P2287S	C7124T	4055; 4205; 4249	100	Yes
orf1ab	A2554V	C7926T	4055; 4204; 4205; 4249	100	Yes
orf1ab	T2823I	C8733T	4205	100	Yes
orf1ab	V2930L	G9053T	4055; 4204; 4205; 4249	100	Yes
orf1ab	L3116F	C9611T	4205	99.1	Yes
orf1ab	T3255I	C10029T	4055; 4204; 4205; 4249	100	Yes
orf1ab	L3606F	G11083T	4204; 4205; 4249	100	Yes
orf1ab	T3646A	A11201G	4055; 4204; 4205; 4249	100	Yes
orf1ab	T4467I	C13665T	4205	98.5	Yes
orf1ab	I4562M	A13951G	4249	35.9	No
orf1ab	N4583K	T14014G	4055; 4204; 4205; 4249	100	Yes
orf1ab	H5401Y	C16466T	4055; 4204; 4205; 4249	100	Yes
orf1ab	I6162T	T18750C	4055; 4249	99.7	Yes
orf1ab	T6249I	C19011T	4205	99.7	Yes
orf1ab	V6265A	T19059C	4249	37.5	No
orf1ab	T6436I	C19572T	4205	100	Yes
orf1ab	T6775I	C20589T	4055; 4205	100	Yes
S	T19R	C21618G	4055; 4204; 4205; 4249	100	Yes
S	T22I	C21627T	4055; 4204; 4205; 4249	100	Yes

S	A27V	C21642T	4055; 4249	100	Yes
S	G142D	G21987A	4055; 4249	57.6	No
S	E156G, ΔFR157-158	GAGTTCA22028G	4055; 4205; 4249	100	Yes
S	L452R	T22917G	4055; 4205; 4249	100	Yes
S	T478K	C22995A	4055; 4249	100	Yes
S	D614G	A23403G	4055; 4204; 4205; 4249	100	Yes
S	P681R	C23604G	4055; 4204; 4205; 4249	100	Yes
S	D950N	G24410A	4055; 4204; 4205; 4249	100	Yes
S	G1085R	G24815A	4055; 4204; 4205; 4249	100	Yes
S	T1117I	C24912T	4249	35.0	No
ORF3a	T12I	C25427T	4205	99.9	Yes
ORF3a	S26L	C25469T	4055; 4204; 4205; 4249	100	Yes
ORF3a	R134H	G25793A	4055; 4205; 4249	100	Yes
M	I82T	T26767C	4055; 4204; 4205; 4249	100	Yes
ORF7a	T39I	C27509T	4204; 4205	100	Yes
ORF7a	V82A	T27638C	4055; 4205; 4249	100	Yes
ORF7a	T120I	C27752T	4055; 4205; 4249	100	Yes
ORF8	S43F	C28021T	4249	29.9	No
ORF8	L60F, Δ61-66	TGTGCGTGGATGAGGCTGG28072T	4205	59.3	No
ORF8	L60F	G28073T	4055; 4249	100	Yes
ORF8	S67*, ΔK68	TCTA28092T	4205	95.6	Yes
ORF8	ΔDF119-120	AGATTTC28247A	4055; 4205; 4249	87.2	Yes
ORF8	F120L	C28253A	4055; 4249	100	Yes
N	D63G	A28461G	4055; 4204; 4205; 4249	100	Yes
N	R203M	G28881T	4055; 4204; 4205; 4249	100	Yes
N	G215C	G28916T	4055; 4204; 4205; 4249	100	Yes
N	D377Y	G29402T	4055; 4204; 4205; 4249	100	Yes

* Notably, 4055, 4205, and 4249 were confirmed positive via the Canadian Food Inspection Agency SARS-CoV-2 PCR.

† The maximum allele fraction for each variant observed in all sequenced samples was calculated from the number of alternate allele observations divided by the total number of observations for each variant site.

‡ A variant with an allele fraction of at least 0.75 or 75% was classified as a major variant.

Figure 1. Map of southern Québec administrative regions and corresponding identification numbers within the study region. Inset shows location of Québec (outlined) and study region (shaded black) within Canada.

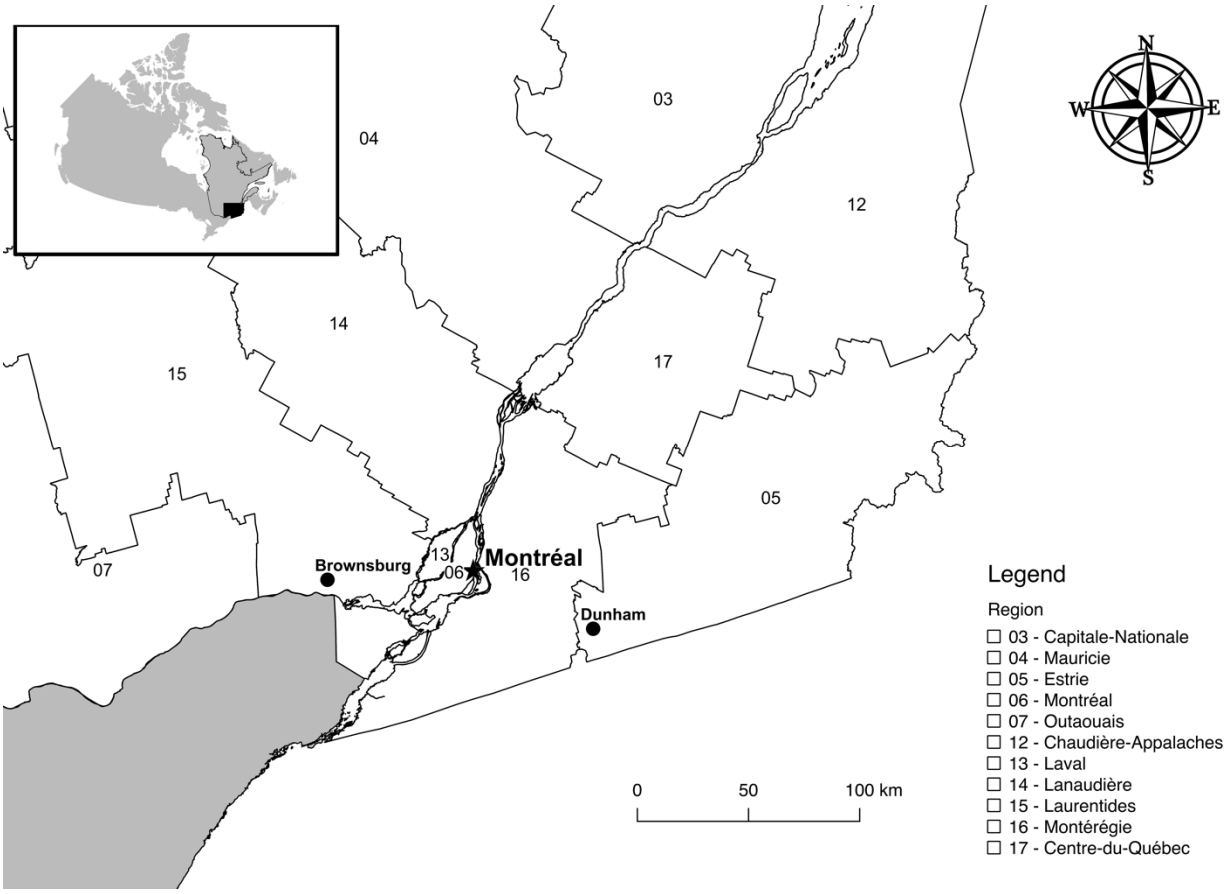

Figure 2. Map of southern Québec with the locations of confirmed SARS-CoV-2 PCR positive (red), serology positive (yellow), and PCR and serology negative (grey) white-tailed deer from November 6 - 8 2021. Infection and exposure data are superimposed on (A) a choropleth map of human population density (per km^2) by regional county municipalities (thin grey boundaries) and (B) a heatmap of deer harvest density per $100km^2$ from 2020 as a proxy for deer population density. Administrative regions are indicated by black boundaries (Figure 1).

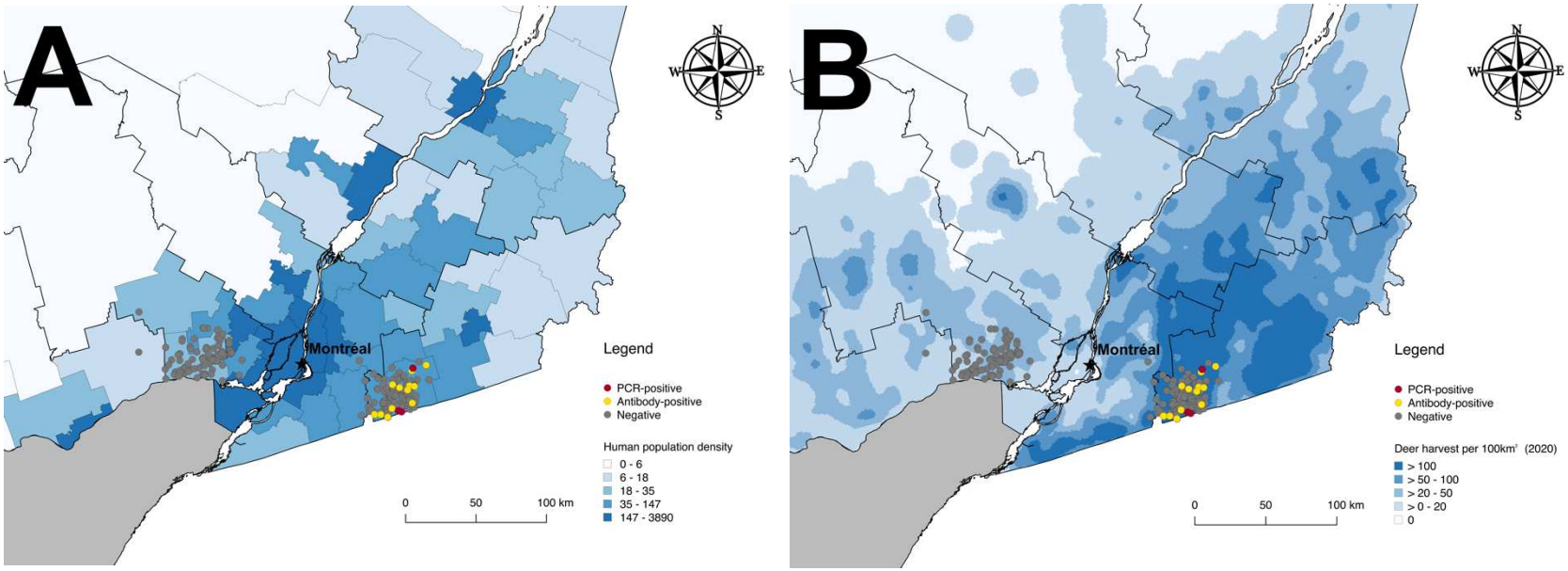

Figure 3. Observed cytopathic effect in VeroE6 cells inoculated with nasal swabs from SARS-CoV-2 positive white-tailed deer at 5 days post infection (A-4055, B-4249) with a mock inoculated negative control (C) and positive control inoculated with a nasopharyngeal clinical specimen from a COVID-19 patient (D). Magnification was 100x.

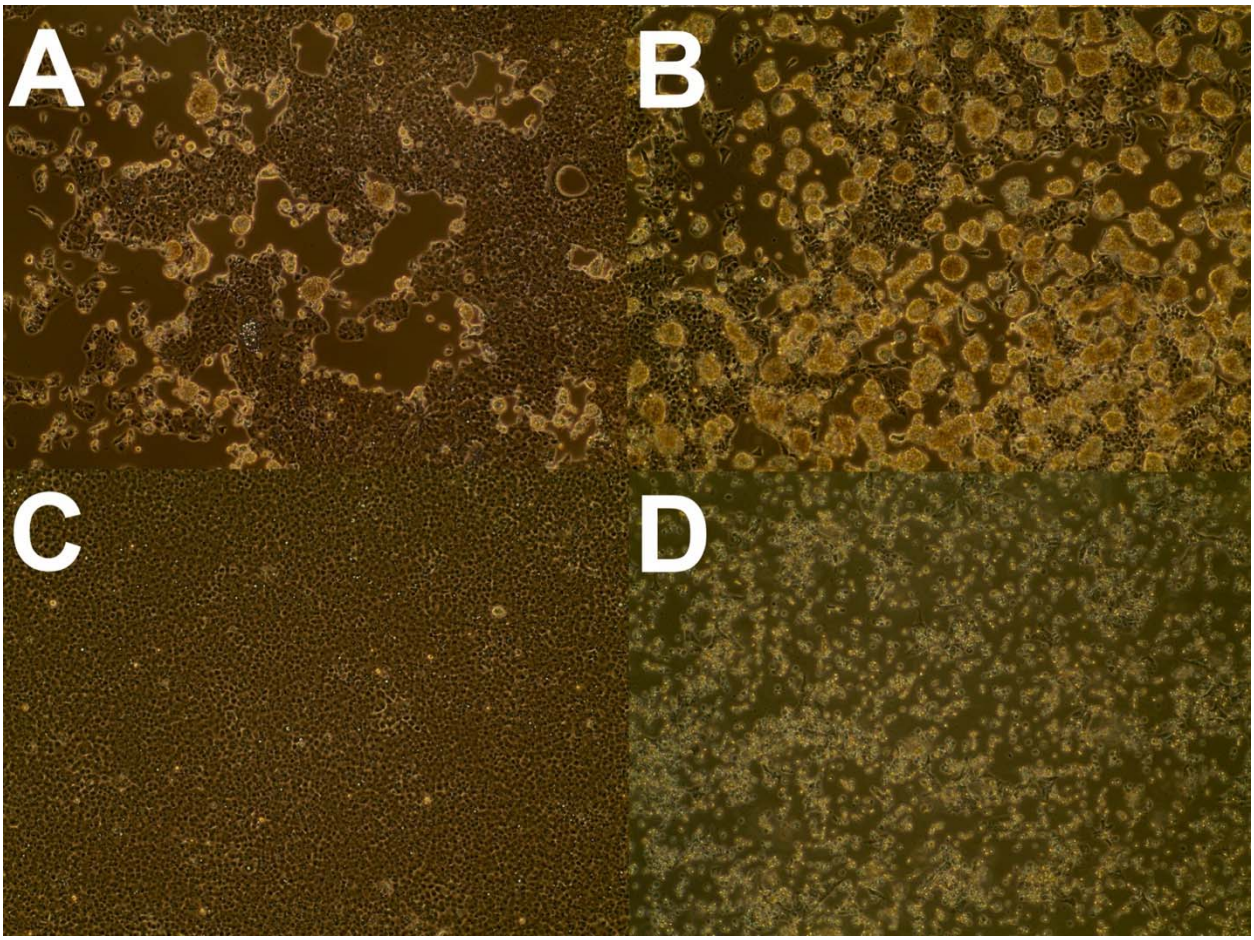

Figure 4. Whole-genome phylogenetic tree of four presumptive SARS-CoV-2 positive white-tailed deer sequences, 45 most closely related Canadian and American GISAID sequences from Pangolin lineage AY.44 and Wuhan-Hu-1 (MN908947.3) reference strain. The CFIA-NCFAD/scovtree Nextflow workflow was used to perform Pangolin lineage assignment, GISAID sequence filtering, Nextalign multiple sequence alignment, IQ-TREE maximum-likelihood phylogenetic tree inference, tree pruning, and visualization with shiptv and Phylocanvas. GISAID sequences (downloaded 2021-12-14; 6,048,277 sequences total) were filtered to select Canadian and USA AY.44 sequences (n=97,470). MSA of filtered GISAID sequences, white-tailed deer sequences and Wuhan-Hu-1 reference sequence was down-sampled to 20,000 sequences for IQ-TREE analysis due to runtime and memory usage constraints. IQ-TREE phylogenetic tree with 20,000 taxa was pruned to 50 taxa total, including only the most closely related taxa to the white-tailed deer sequences, for visualization. Amino acid (AA) substitutions and deletions in GISAID and white-tailed deer sequences were determined using Nextclade for visualization alongside the tree and other metadata. Only notable S gene AA mutations present or absent in the white-tailed deer sequences are highlighted. Some positions within the S gene for sample 4204 had low or no coverage, however, despite the poor coverage of sample 4204, it still clustered with the other white-tailed deer sequences.